Neuron, Vol. 31, 409–420, August 16, 2001, Copyright ©2001 by Cell Press

The CRE/CREB Pathway Is Transiently Expressed in Thalamic Circuit Development and Contributes to Refinement of Retinogeniculate Axons

Tony A. Pham,[1,6] John L. R. Rubenstein,[4] Alcino J. Silva,[5] Daniel R. Storm,[2] and Michael P. Stryker[3]

[1] Departments of Psychiatry and Behavioral Sciences and Ophthalmology
Graduate Program in Neurobiology and Behavior
[2] Department of Pharmacology
University of Washington School of Medicine
Seattle, Washington 98195
[3] Department of Physiology
[4] Department of Psychiatry
University of California, San Francisco
San Francisco, California 94143
[5] Departments of Neurobiology, Psychiatry, and Psychology
University of California, Los Angeles
Los Angeles, California 90095

Summary

The development of precise connections in the mammalian brain proceeds through refinement of initially diffuse patterns, a process that occurs largely within critical developmental windows. To elucidate the molecular pathways that orchestrate these early periods of circuit remodeling, we have examined the role of a calcium- and cAMP-regulated transcriptional pathway. We show that there is a window of CRE/CREB-mediated gene expression in the developing thalamus, which precedes neocortical expression. In the LGN, this wave of gene expression occurs prior to visual experience, but requires retinal function. Mutant mice with reduced CREB expression show loss of refinement of retinogeniculate projections. These results suggest an important role of the CRE/CREB transcriptional pathway in the coordination of experience-independent circuit remodeling during forebrain development.

Introduction

The brain functions of higher organisms, and their underlying neural circuitry, develop gradually through a combination of intrinsically driven and sensory experience-dependent mechanisms. During the early stages, genetically specified molecular cues direct the formation of connections between the major centers of the mammalian brain, but these initial connections are often diffuse, lacking the network precision necessary to process complex information. A gradual process of remodeling then occurs that gives rise to the precision of mature connections. In the mammalian brain, circuit remodeling is an extended process that occurs in progressive stages within different brain regions (for review, see Katz and Shatz, 1996). Studies of primary sensory systems, which have served as models for understanding functional brain development, have provided clear evidence for windows of plasticity and remodeling (Fox and Zahs, 1994; Hubel and Wiesel, 1998). However, the mechanisms that orchestrate these critical phases of circuit development remain largely unclear.

In the visual system of cats, thalamocortical projections representing each of the two eyes, which are initially diffuse, segregate into distinct zones in the visual cortex during the first few weeks of life (LeVay et al., 1978). During and shortly following this period of remodeling, the functional connectivity of neurons in the visual cortex is extraordinarily responsive to visual deprivations (Hubel and Wiesel, 1970; Wiesel and Hubel, 1963b). A critical phase of remodeling and plasticity is observed also in the dorsal thalamus, a subcortical structure that feeds incoming sensory information to the neocortex. In mammals, retinal axons from both eyes innervate each dorsal lateral geniculate nucleus (dLGN). During development, when the retinal axons first reach the dLGN, sets of axons originating from each eye are initially intermingled. Through a gradual process of refinement, involving the elimination of inappropriate projections and branches and the selective growth of correct projections, the two sets of retinogeniculate axons become segregated, thereby innervating distinct layers of the LGN (Sretavan and Shatz, 1986a). This refinement of retinogeniculate connections involves competitive interactions between the two eyes. When one retina is removed (or its activity silenced by tetrodotoxin injections) early in development, the remaining eye's ipsilateral axonal projections spread outward to occupy a larger area within the LGN (Godement et al., 1987; Penn et al., 1998; Rakic, 1981; Sretavan and Shatz, 1986b). Interestingly, the period of plasticity of subcortical connections ends much earlier than that of cortical connections. Retinogeniculate plasticity is confined to the prenatal or neonatal period (Guillery, 1972; Robson et al., 1978). In contrast, visual cortical plasticity can be observed past one month of life in a number of mammalian species, including the mouse (Blakemore et al., 1978; Gordon and Stryker, 1996; Hubel and Wiesel, 1970). In addition, significant plasticity of intracortical connections exists at even older ages in the absence of thalamocortical plasticity (Darian-Smith and Gilbert, 1995; Fox, 1994). Therefore, there are developmental mechanisms that orchestrate the timing of remodeling and plasticity of neural connections in the mammalian brain, but the mechanisms underlying these critical windows remain poorly understood.

Several candidate molecular systems have emerged that may be critical in the regulation of critical periods of development, including the NMDA receptor (Fox et al., 1991; Tsumoto et al., 1987), the neurotrophin BDNF (Hanover et al., 1999; Huang et al., 1999), and GABA-mediated inhibitory circuitry (Fagiolini and Hensch, 2000). More recently, *class I MHC* genes (Corriveau et al., 1998), the activity-regulated gene *cpg15* (Corriveau et al., 1999), and modulatory neurotransmitter systems (Upton et al., 1999) have also been implicated. However, it remains unclear how these systems are integrated

[6] Correspondence: tonypham@u.washington.edu

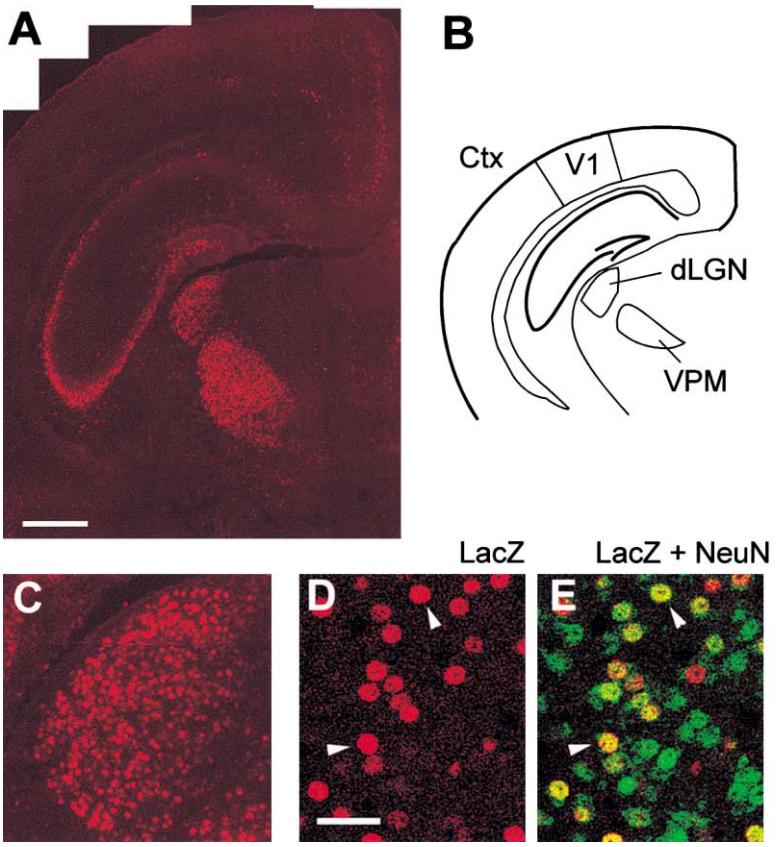

Figure 1. The CRE/CREB Transcriptional Pathway Is Constitutively Active in the Mouse Forebrain during the Early Postnatal Period

(A and B) At postnatal age 4 days (P4), there is robust CRE-mediated gene expression in the dorsal thalamus and hippocampus of CRE-*lacZ* reporter mice. This is illustrated in a composite of confocal microscope images of a 16 μm coronal section stained for lacZ immunofluorescence (A), which corresponds to the schematic (B) showing locations of the relevant structures. Abbreviations: H, hippocampus; V1, primary visual cortex; dLGN, dorsal lateral geniculate nucleus; VPM, ventral posteromedial nucleus. Scale bar = 0.5 mm.

(C–E) Higher magnification images showing cells within the dLGN. By colabeling histologic sections using an antibody against a neural-specific marker (NeuN) (D and E), we find that lacZ-expressing cells (red) colocalize with NeuN-containing cells (green). Cells with double-labeling are yellow (examples marked by arrowheads in [D] and [E]). Scale bar = 25 μm for (D) and (E.)

in the expression of critical period plasticity and the temporal regulation of its emergence and disappearance within different brain regions. A powerful cellular mechanism that has not been examined in detail in this context is genetic control at the transcriptional level. Yet, a large number of studies have shown that master transcriptional control of gene expression lies at the heart of nearly every key developmental transition, including the control of body and nervous system regionalization (for example, see Rubenstein et al., 1994) and the regulation of cellular differentiation in diverse organ systems.

A candidate nuclear pathway that might be critical in the developmental control of neural plasticity in the mammalian brain is the cAMP responsive element (CRE)/CREB transcriptional pathway (for review, see Silva et al., 1998). The CRE binding protein (CREB) is a calcium- and cAMP-regulated transcriptional activating protein that is responsive to neural activity patterns. CREB is required for consolidation of long-lasting plasticity and memory formation in nearly all neural systems examined thus far, including *Aplysia*, *Drosophila*, and mouse (Bourtchuladze et al., 1994; Casadio et al., 1999; Yin et al., 1994). Activity-dependent synaptic mechanisms that underlie adult memory and learning are hypothesized to function also during circuit development. And yet, the regulation and functions of CREB during brain development have not been described.

In this report, we examine the function of CREB and CRE-mediated gene expression during development of synaptic circuitry in the dorsal thalamus. Our results indicate that there is a well-defined window of CREB activation and CRE-mediated gene expression during development of the thalamus, coincident with the period of refinement of thalamic connections. In addition, using *CREB* mutant mice, we show that *CREB* is important for accurate refinement of retinogeniculate projections. Taken altogether, these results suggest a role for the CREB transcriptional pathway in the coordination of circuit remodeling prior to sensory experience.

Results

The CRE/CREB Transcriptional Pathway Is Activated at Specific Sites in the Postnatal Developing Forebrain

To examine the function of the CREB family of transcriptional regulators acting on CREs during development, we used transgenic mice carrying a CRE-*lacZ* reporter gene (Impey et al., 1996). This in vivo reporter system has been shown to be responsive to calcium and cAMP in brain slices (Impey et al., 1996; Impey et al., 1998a) and to be upregulated during experience-dependent neural plasticity (Barth et al., 2000; Impey et al., 1998b; Pham et al., 1999). As shown in Figure 1, there is robust expression of lacZ in these mice in discrete regions of the developing forebrain at postnatal day 4. Intense CRE-mediated gene expression can be observed in the dorsal lateral geniculate nucleus (dLGN) and the ventral posteromedial nucleus (VPM), dorsal thalamic nuclei that receive visual and somatosensory inputs, respectively. Robust expression can also be seen in the hippocam-

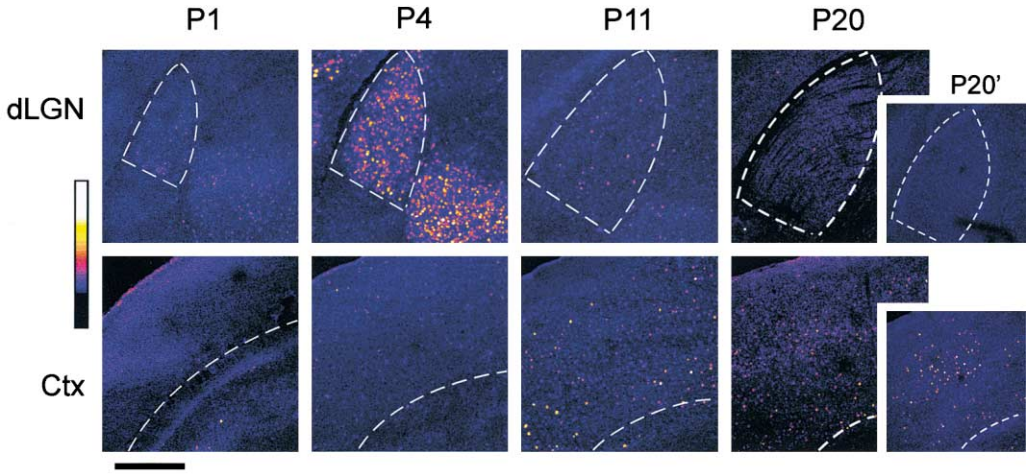

Figure 2. CRE-Mediated Gene Expression Appears Transiently in the dLGN during Postnatal Development

Coronal sections from CRE-*lacZ* mice of various developmental stages were labeled for lacZ, imaged on a confocal microscope, and shown here rendered in a color scale representing fluorescence intensity. For all age groups, images of the dLGN and visual cortex (Ctx) are taken from the same section. All images were taken during one imaging session, using identical confocal settings. Panels labeled P1 through P20 show representative results (n = 4 mice for P1–P11, n = 10 for P18–P20). Panel P20′ shows an atypical case where robust cortical CRE-*lacZ* staining was observed, but even here no significant dLGN expression could be observed.

pus, particularly in the CA3 region. Much lighter expression exists elsewhere, and in particular only scattered, lightly-stained cells can be seen in the neocortex (here, visual cortex). Within the dLGN, many cells can be seen to express *lacZ* (Figure 1C). To determine whether these cells are neurons, we labeled sections for lacZ and NeuN, a neuron-specific marker. As shown in Figures 1D and 1E, almost all lacZ-positive cells also stain for NeuN (yellow cells in panel E). This finding indicates that CRE-mediated gene expression in the dLGN occurs within neurons. Because CREB is thought to be a ubiquitous transcription regulatory factor, the finding that CRE-mediated gene expression is heavily localized seems surprising and suggests precise spatiotemporal regulation of CREB function within the brain.

To characterize the developmental role of the CREB pathway further, we decided to focus on the dorsal thalamus, specifically the dLGN, because inputs to the dLGN have been characterized and are known to undergo dramatic remodeling during development (Godement et al., 1984). At around the time of birth, the ipsilateral retinal axons begin to innervate the dLGN. Initially, these ipsilateral projections intermingle and overlap with the contralateral projections, which began arriving at the dLGN several days earlier (prior to birth). From P2 to P8, remodeling of retinogeniculate projections occurs, which results in partial segregation of these inputs within the dLGN (Godement et al., 1984).

To determine the temporal regulation of the CREB transcriptional pathway in the dLGN, we examined expression of the CRE-*lacZ* reporter during early postnatal development. Figure 2 shows lacZ immunofluorescence in the dLGN (upper panels) and visual cortex (lower panels) from postnatal days 1 through 20. At P1, there is a low level of *lacZ* expression in the LGN, which rises dramatically by P4 and then falls off rapidly after the first week. By P20, only background lacZ immunostaining can be observed in the dLGN. In contrast, areas of visual cortex contained within the same sections as those shown in the upper panels show little lacZ expression until about P11. Figure panels representing ages P1–P20 show representative results (n = 4 animals for P1–P11, n = 10 for P18–P20). At age P18–P20, a minority of the mice (two of ten) showed strong neocortical expression (panel P20′), but even these displayed no significant dLGN expression. These results indicate that there is differential regulation of CRE-mediated gene expression in the dorsal thalamus as compared to the cortex, with transient expression in the dLGN and delayed onset in the visual cortex.

CREB Protein Expression Is Regulated during Dorsal Thalamus Development

The spatiotemporal regulation of CRE-mediated gene expression indicates that transcriptional regulatory components such as CREB and associated proteins may be developmentally expressed and/or activated. Thus, we examined the regulation of CREB expression in the developing dorsal thalamus by immunohistochemistry and by Western immunoblotting. Figure 3A shows confocal microscope images of CREB immunofluorescence in the dLGN at different postnatal stages. The results show that CREB immunoreactivity is present at birth, rises during the first week, and then drops significantly by 20 days of age. Western immunoblot analysis (Figures 3B and 3C) using protein extracts from dorsal thalamus confirms that CREB is downregulated with maturation. Here, identical amounts of total protein were loaded onto each lane. By densitometric quantification of chemiluminescence signal exposed on film, we find that at P20 CREB immunoreactivity has declined to about 25% of its level at P1. To test for statistical significance, the ANOVA test was performed, which revealed that the four age groups are significantly different [$F(3,10) = 10.18$, $p = 0.002$]. Specifically, there is a significant negative linear trend of CREB expression as a

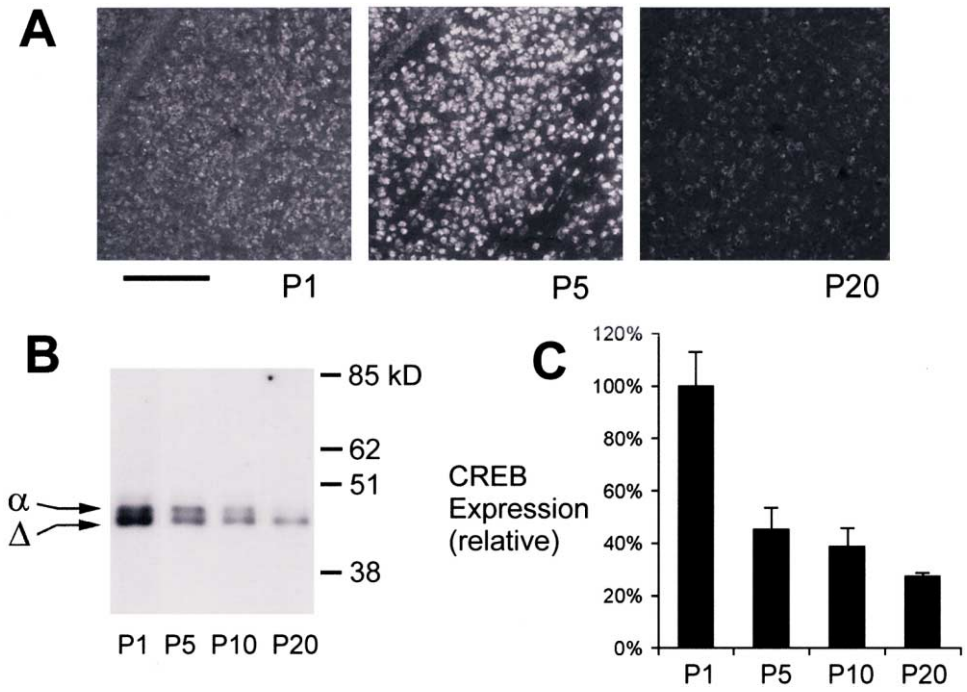

Figure 3. Expression of CREB and CREB Isoforms Is Strongly Modulated during dLGN Development

(A) Fluorescence immunohistochemistry shows strong expression of CREB in the dLGN shortly after birth, which declines with maturation. Histologic sections from mice of ages P1, P5, and P21 were processed for immunofluorescence using a CREB polyclonal antibody. All of these sections were processed in tandem and imaged using identical confocal microscope settings. Three animals were examined for each group. Scale bar = 0.15 mm

(B and C) Western blotting reveals differential expression of CREB α and Δ isoforms during postnatal development (B). Both isoforms are initially expressed at nearly equal levels and are downregulated with age. However, with maturation the α isoform is downregulated more strongly relative to the Δ isoform, which predominates at P20. Equal amounts of total protein extracts from dorsal thalamus were loaded onto each lane, blotted, and probed with a CREB polyclonal antibody. Quantification of total CREB expression (α and Δ isoforms) was performed by densitometric scanning (C). The relative average value in each age group examined are shown (n = 5 animals for P1, n = 3 animals for P5–P20). Error bars in (C) represent the SEM.

function of age [$F(1,10) = 25.71$, $p < 0.001$]. Surprisingly, the Western blot result suggests a lower expression of CREB at P5 as compared to P1, while immunofluorescence detects higher levels of staining in nuclei at P5. One reason for this difference could be that Western blotting is normalized to total protein, while immunohistochemistry results are not normalized but instead show absolute CREB expression present in histologic sections. Thus, changes in CREB expression relative to other cellular proteins during development might cause differences in results. Another important difference is that protein conformations and protein-protein interactions are preserved in immunohistochemistry with fixed sections, while they are lost during Western blotting. In any case, both methods indicate that CREB protein levels decline significantly with maturation.

Perhaps more intriguing, we found that there is differential regulation of CREB isoforms during postnatal development. During the period from P1 to P20, we observed expression of two CREB isoforms, which match the molecular weights for previously described CREBΔ and CREBα (Figure 3B) (Blendy et al., 1996; Ruppert et al., 1992). Consistent with prior studies using adult brain tissue, we found that at P20 CREBΔ is by far the predominant isoform. However, at earlier stages CREBα is expressed much more highly, and its expression equals that of CREBΔ at P5. These results are novel, and they suggest the possibility of differential gene regulation by CREBΔ and CREBα isoforms during mammalian brain development.

The activity of CREB requires its phosphorylation on serine residue 133, which potentiates the binding of CREB to DNA and to coactivator proteins (for review, see Montminy, 1997). To determine whether phospho-CREB is present during thalamus development, we examined the spatiotemporal distribution of phospho-CREB by fluorescence immunohistochemistry. Our results (Figure 4A) show that at P5, phospho-CREB is present widely in the forebrain, but in posterior forebrain sections it is found at highest levels in the dorsal thalamus and the hippocampus. There is a striking temporal regulation over the course of dLGN development, as shown in Figures 4B–4D. Phospho-CREB immunoreactivity is present at P1, rises during the first postnatal week, and then drops dramatically afterward. By P21, little if any phospho-CREB immunoreactivity can be detected above the background. This pattern closely resembles that of total CREB (Figure 3A), and it is possible that the regulation of phospho-CREB observed here is entirely at the level of CREB protein. Nonetheless, these results are in agreement with the results obtained using the CRE-*lacZ* reporter and show that active CREB is

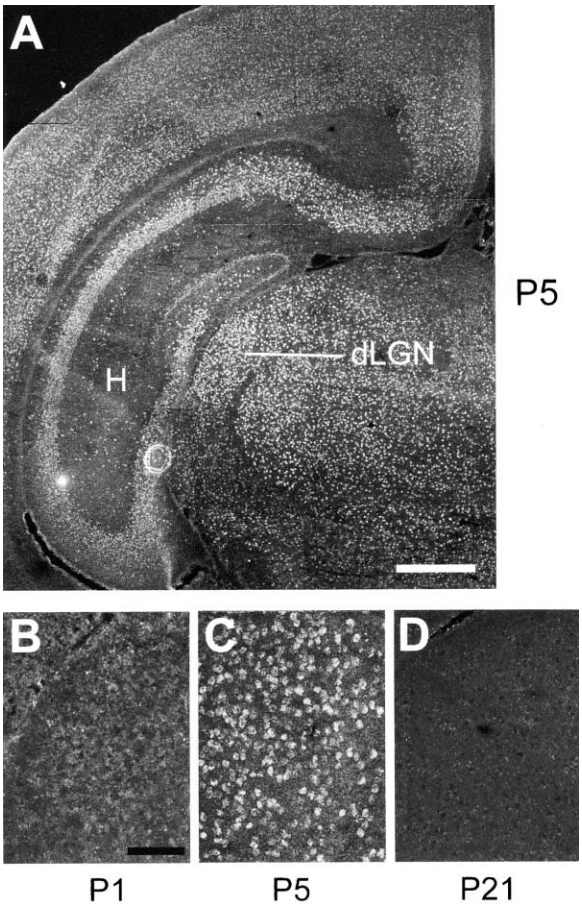

Figure 4. Phospho-CREB Is Restricted to Early Postnatal Development of the dLGN

At postnatal age 5 days, phospho-CREB (Ser-133) can be detected in most regions of the forebrain, including abundant amounts in the dLGN, hippocampus, and parts of the neocortex. This is illustrated in (A), which is a composite of multiple confocal microscope images of phospho-CREB immunofluorescence. In the dLGN, low levels of phospho-CREB is found at P1 (B), but it becomes clearly detectable by P5 (C), and declines to below background levels by P21 (D). Abbreviation: H, hippocampus. Scale bar = 0.5 mm (A); 0.1 mm (B–D).

found transiently during postnatal thalamus development.

CRE-Mediated Gene Expression in the Developing dLGN Is Modulated by Retinal Activity Prior to Eye Opening

Although eye opening does not occur until 12–14 days after birth, it is possible that spontaneous retinal activity (Galli and Maffei, 1988; Wong, 1999) drives CRE-mediated gene expression in the LGN during early postnatal development. To examine whether retinal function may be required for CRE-mediated gene expression in the dLGN, we enucleated one eye of CRE-*lacZ* mice at P4–P5 and then examined *lacZ* expression 24 hr later. Figure 5 shows lacZ (A and B) and phospho-CREB (C and D) immunofluorescence in the left and right dLGN for mice that received monocular enucleation. The anatomic correspondence of the dLGN with respect to the

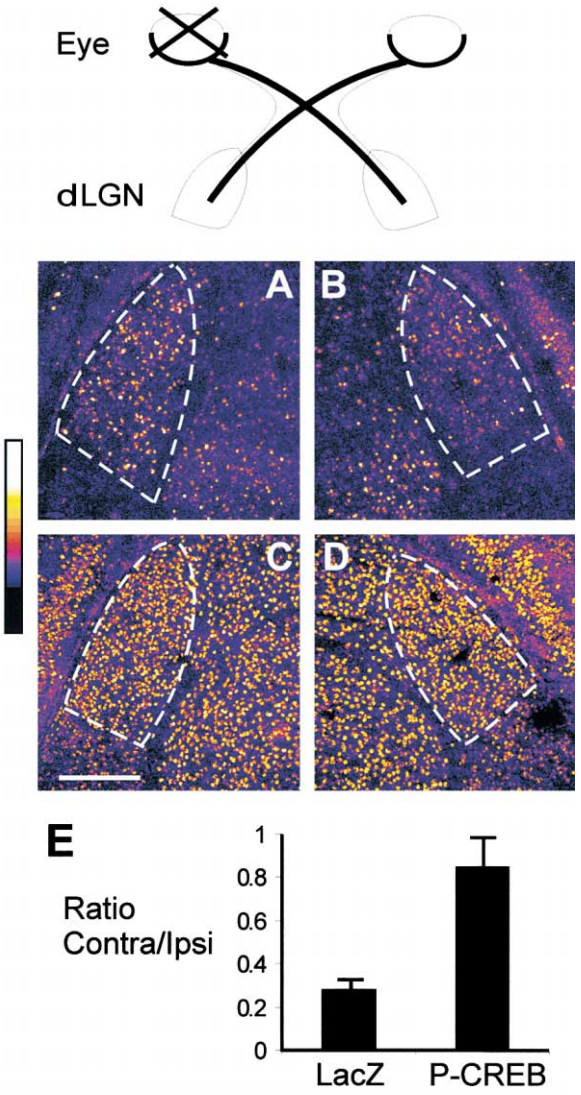

Figure 5. Retinal Function Is Critical for CRE-Mediated Gene Expression in the dLGN

(A–D) When the retina is removed by enucleation, CRE-*lacZ* expression (A and B) but not phospho-CREB immunoreactivity (C and D) decreases significantly in the dLGN. The schematic depicts the retinogeniculate pathway and serves to orient (A)–(D) to the enucleated and intact pathways. Mice were monocularly enucleated at P5 and then sacrificed at P6. Histologic sections were then stained for lacZ or phospho-CREB by using indirect immunofluorescence, and then imaged on a confocal microscope. As shown in the schematic, retinal axons primarily project contralaterally, and therefore the effects of enucleation can be determined by comparing lacZ expression in the ipsilateral and contralateral dLGN. Scale bar = 0.3 mm (E) When results are quantified by counting cells, we find that the dLGN contralateral to the enucleated eye has 28% of lacZ-expressing cells found in the ipsilateral dLGN (contralateral/ipsilateral ratio of 0.28). For phospho-CREB, the contra/ipsi cell ratio is 0.85. Error bars denote the SEM. n = 4 animals for lacZ; n = 3 animals for phospho-CREB.

enucleated eye is shown in the schematic diagram above the figure panels. Because greater than 90% of retinal axons innervate the contralateral eye, the effects of monocular enucleation should be much greater in the contralateral eye compared to the ipsilateral eye. Our

results indicate that there is a strong reduction in CRE-*lacZ* gene expression following enucleation, when the contralateral dLGN (Figure 5B) is compared to the ipsilateral dLGN (Figure 5A). When results were quantified by counting cells that show robust lacZ staining (Figure 5E), we found that enucleation causes reduction of lacZ positive cells in the dLGN contralateral to the enucleated eye, to 28% of the number found in the opposite (ipsilateral) dLGN (95% confidence interval = ±13%).

In contrast to the effects observed with CRE-mediated gene expression, we found that enucleation had no impact on phospho(Ser-133)-CREB levels. As depicted in Figures 5C and 5D, dLGNs contralateral or ipsilateral to the enucleated eye show very similar phospho-CREB distributions. When cells that express phospho-CREB were counted (Figure 5E), we observed that the dLGN contralateral to the enucleated eye has 85% of the number of the ipsilateral dLGN (95% confidence interval = ±31%). Therefore, although phosphorylation of Ser-133 is required for CREB function, it is likely not dependent on retinal activity, nor is it sufficient for CRE-mediated gene expression. This is consistent with various other reports in the literature showing that CREB phosphorylation is necessary but not sufficient for CRE-mediated transcription (for examples, see Hardingham et al., 1999; Hu et al., 1999). Presumably, activation of other components of the CREB pathway is also critical.

CREB Mutant Mice Show Smaller dLGN Size but Normal Gross Brain Morphology

To examine the role of CREB during forebrain development, we first examined Nissl-stained histologic sections of P10 mice. Figures 6A and 6B show low magnification images of coronal sections through the posterior part of the brain. The major structures of the brain, including the neocortex, hippocampus, dentate gyrus, thalamus, and corpus callosum, appear grossly normal. However, we note that the corpus callosum often appears smaller in the mutants; a similar observation was previously reported for *CREB* null mice (Rudolph et al., 1998). The laminar organization of cells in the mutant and control neocortex appears indistinguishable from each other. When the dLGNs were viewed under higher magnification (Figures 6C and 6D), no obvious structural differences between the mutants and controls could be detected. However, the dLGNs of the mutant mice are significantly smaller. The mutant dLGNs are smaller in cross-sectional area, and they span fewer coronal sections. To determine the magnitude of these differences, we measured the area of the dLGN as defined by the boundaries of retinogeniculate projections, using images similar to those shown in Figures 7E and 7G. The mean cross-sectional dLGN area was determined by averaging values for three sections through the center region of the dLGN (where the dLGN is the widest). As shown in Figure 6E, the mutant dLGN size was approximately 23% smaller than that for controls ($p < 0.01$, Student's t test). To determine whether the mutant dLGNs might contain the same number of cells, despite the size differences, we measured the cell density within a defined area in the dorsolateral quadrant of the dLGN. We found that the average cell density is virtually identical between mutant and controls (Figure 6F) ($p = 0.83$, Student's t test). For controls, the average density is defined as 100% (95% confidence interval = ±11.2%), while for mutants the average density is 101% (95% confidence interval = ±5.7%). This analysis indicates that the probability that the cell density of mutants is

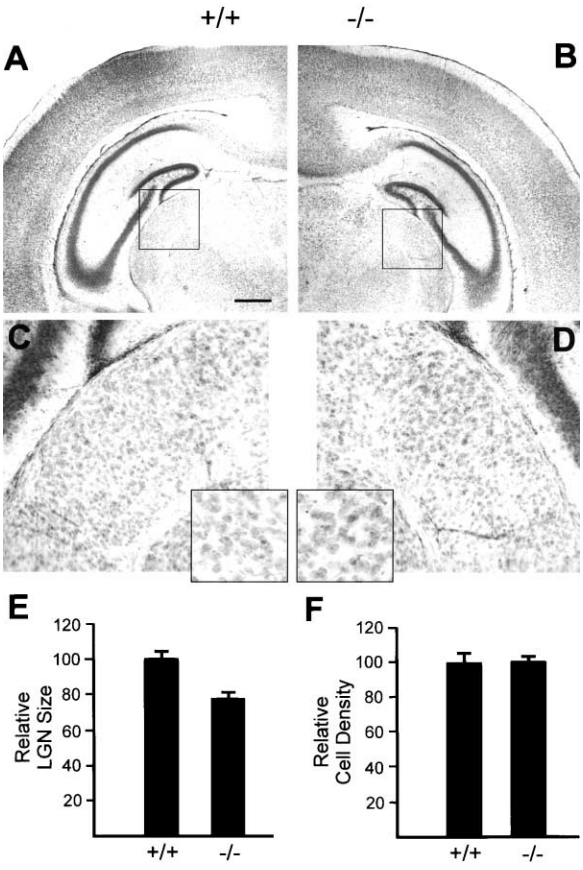

Figure 6. The Gross Brain Morphology of CREB Mutant Mice Is Normal but Shows Smaller dLGN Size

(A–D) To characterize the brain morphology of CREB mutant mice and littermate controls, coronal sections of P10 mice were stained with cresyl violet. At low magnification, the major brain structures of mutant mice are intact and appear similar to controls (compare [A] and [B]). The dLGN of mutant mice shows grossly normal distribution of cells, and the cellular morphology is not distinguishably different from controls (compare [C] and [D]). Scale bar = 0.5 mm for (A) and (B).

(E and F) Quantification of dLGN size (E) reveals that the dLGN of mutant mice is about 20% smaller than controls ($p < 0.01$, Student's t test). The average LGN cross-sectional area for mutant (0.20 mm^2) and wild-type (0.26 mm^2) animals were determined from coronal sections through the center of the LGN. Because it is difficult to delineate the boundary of the dLGN precisely in cresyl violet-stained sections, areal measurements were derived from the distribution of the contralateral retinogeniculate projections (shown in Figure 6). Measurements were made from three coronal sections per animal, then averaged. To determine whether the cell density in the dLGN of mutant mice is different from controls, cells were counted in a defined representative area of the dLGN and expressed here as a percentage of the wild-type average (F). The cell density is indistinguishable between mutants and controls ($p = 0.83$, Student's t test). Results represent data from four mutants and four littermate controls. Error bars depict the SEM.

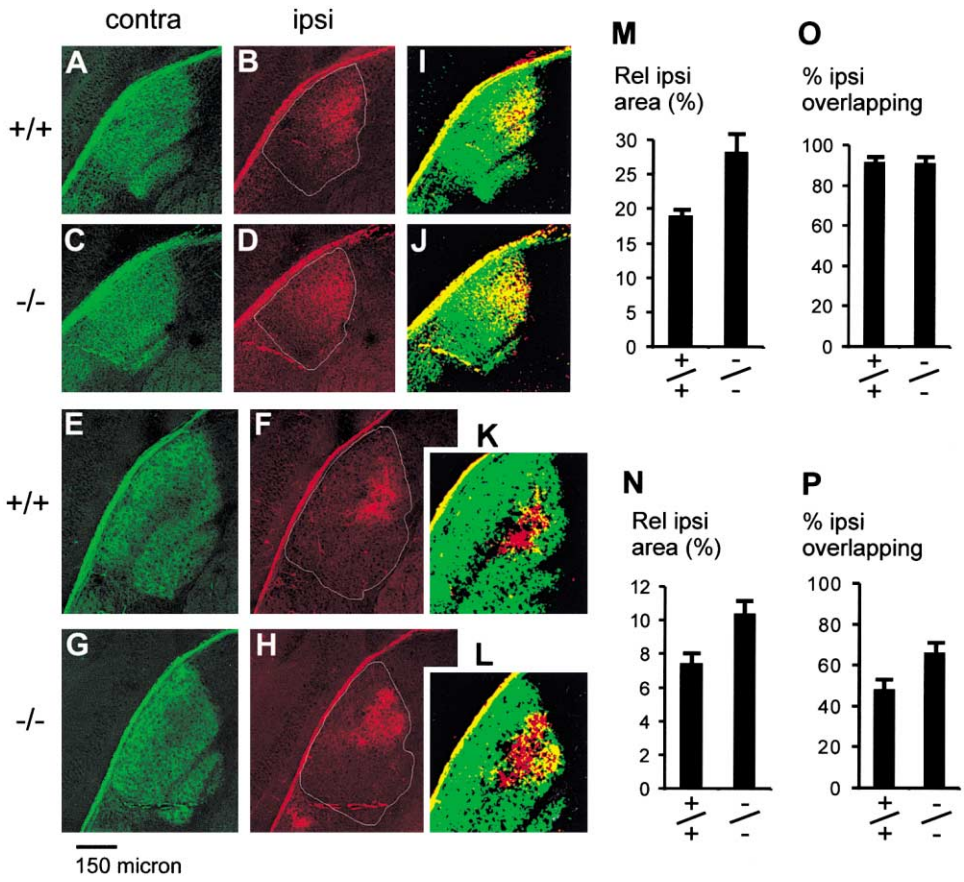

Figure 7. CREB Hypomorphic Mice Show Loss of Refinement of Retinogeniculate Projections

By labeling the retinogeniculate axons with fluorescent dyes, the patterning of ipsilateral and contralateral retinal projections was determined and quantified. Shown are labeled contralateral (green) and ipsilateral (red) retinal projections in the dLGN of wild-type (+/+) and homozygous hypomorphic mice (−/−), as imaged by confocal microscopy. (A)–(D), (I), (J), (M), and (O) represent P5 age group. (E)–(H), (K), (L), (N), and (P) represent P10 age group.

(A–D) Retinogeniculate projections at age P5. At this age, the projections are diffuse and the ipsilateral and contralateral projections can be seen to overlap extensively. Ipsilateral projections of mutant mice are typically larger than those of wild-type mice.

(E–H) Retinogeniculate projections at age P10. Significant refinement can be seen, compared to age P5. However, the ipsilateral projections of mutant animals remain more diffuse than those of wild-type animals.

(I–L) Representation of overlap of ipsilateral and contralateral axons. Images were smoothed to removed pixilated noise, and thresholded as described in Experimental Procedures. Axonal projections exceeding defined threshold levels are encoded in green (contralateral) and red (ipsilateral). Overlap areas are shown in yellow.

(M and N) Quantification of relative ipsilateral areas in CREB mutant mice and wild-type controls. Average relative areas for all animals in each group are shown. Data were obtained from five mutants and three littermate control animals for P5 group (M), and four mutants and four controls for P10 group (N). For both P5 and P10, mutant mice (−/−) show significantly greater relative areas compared to wild-type mice. At P5 the ipsilateral projections of mutant animals are 54% greater than wild-type littermates ($p = 0.02$, ANOVA), while at P10 the mutant projections are 36% greater than controls ($p = 0.01$, ANOVA). Error bars depict the SEM.

(O and P) Quantification of the fraction of the ipsilateral patch that is overlapping at P5 and P10. Average percent of overlap is shown, with error bars depicting the SEM. Analyses were performed using the same data set described above. At P5, mutants and controls show identical overlap, with 91% of the ipsilateral patch overlapping ($p = 1.0$, ANOVA). At P10, wild-type animals show significantly less overlap then mutants ($p = 0.04$, ANOVA).

equal to or greater than 120% of controls is unlikely ($p < 0.05$), and it also implies that the mutant dLGNs contain fewer neurons compared to controls. To determine whether changes in brain size might be a general effect, we measured visual cortical thickness in these same mutant and control mice, using sections containing the center region of the dLGN. This analysis revealed no significant difference between mutants and controls (data not shown). Therefore, these results suggest that there are specific abnormalities in brain morphology of CREB mutant mice, but that the general patterns of brain development are preserved.

CREB Is Important for Accurate Refinement of Retinogeniculate Projections

The expression of the CREB transcriptional pathway during a crucial period of growth and refinement of thalamic connections suggests that CREB might be required for proper development of these connections. Because thalamic function is required for refinement of retinal

projections to the LGN (Sretavan et al., 1988), we hypothesize that CREB function in the LGN might be important for stabilization of presynaptic retinal terminals during refinement. To test this hypothesis, we characterized the development of retinogeniculate projections in transgenic mice deficient in CREB protein, the α,Δ-CREB hypomorphic mice. Although a complete CREB knockout strain exists, these mice do not survive past the day of birth because of pulmonary defects (Rudolph et al., 1998). In using the hypomorphic mice, our reasoning is that although the mutant phenotype would be attenuated, any positive findings would suggest larger roles for CREB than could be observed.

To examine the morphology of retinogeniculate axons in the CREB hypomorphic mice, we labeled separately the projections of the left and right eyes by using different fluorescent dyes. Coronal sections through the middle of the dLGN were imaged by confocal microscopy, revealing the pattern of contralateral and ipsilateral projections within the same dLGN. Figures 7A and 7B show retinogeniculate projections for control mice at postnatal day 5, a stage when considerable remodeling of ipsilateral projections has taken place (although active refinement is still occurring) (Godement et al., 1984). Consistent with published results, the ipsilateral projections at this age form a diffuse patch, limited largely to the medial one-half of the dLGN. The terminals of the contralateral projections, which are far more abundant, cover the entire extent of the dLGN. Figures 7E and 7F depict the contralateral and ipsilateral projections at postnatal day 10, a stage when refinement is complete. Extensive remodeling could be seen in the ipsilateral projections, as evidenced by the organization of the terminals into dense clusters and the retraction of axons away from the edges of the dLGN. At the same time, contralateral axons have thinned markedly from the zone occupied by the ipsilateral projections, resulting in partial segregation of these inputs. When homozygous CREB mutant mice were examined (Figures 7C, 7D, 7G, and 7H), we find that their retinal axons terminated correctly in the dLGN, but within the dLGN the projections appear significantly more diffuse. This can be seen most clearly with the ipsilateral projections. At P5 during the period of active remodeling, the mutant ipsilateral projections cover a more diffuse area of the dLGN, extending toward the dLGN boundaries, compared to the controls. At P10, although both mutant and wild-type projections show considerable refinement, the mutant projections remain significantly more diffuse and cover a larger relative area.

Although the relative size of ipsilateral projections is larger and more diffuse in the CREB mutant mice, we did not find any evidence for errors of targeting of retinal axons. The boundary of the dLGN is clearly defined by the contralateral axons, which actually encompasses a smaller area in the mutant mice. Also, the ipsilateral axons were not observed to terminate outside of the dLGN in the mutant mice, although their pattern is more diffuse within the dLGN.

By superimposing contralateral and ipsilateral projections coded in different colors, the overlap of these sets of projections could be visualized (Figures 7I–7L). In order to clearly show the boundaries of the projections, image pixels containing fluorescence-labeling intensities exceeding a defined threshold value (identical parameters used for wild-type and mutant projections) were coded in green (contralateral) or red (ipsilateral). Areas of overlap of the projections are displayed in yellow. At P5, virtually all of the ipsilateral patch overlaps with contralateral projections. By P10, segregation of the projections could be observed in wild-type mice. However, in the hypomorphic mice, the degree of segregation is significantly less, and greater overlapping areas could be observed. These results suggest that accurate and complete refinement of retinal projections is disrupted in the CREB mutant mice.

To provide a rigorous measure of retinogeniculate refinement seen with mutant and control mice, we quantified the area occupied by the ipsilateral projections relative to the total area of the dLGN, a method used previously by other investigators (Huh et al., 2000; Penn et al., 1998). Five mutants and three littermate control animals were examined at P5; four mutants and four controls were examined at P10. Three central sections through the dLGN were analyzed per animal. Our analysis suggests that there is a loss of refinement in the mutants at both P5 (Figure 7M) and P10 (Figure 7N). For P5 mice, the average relative ipsilateral projection size was about 50% greater in the mutants ($p = 0.02$, ANOVA). For the P10 mice, the average relative area covered by the ipsilateral projections was 36% greater in the homozygous mutants compared to wild-type controls ($p = 0.01$, ANOVA). Heterozygous animals showed intermediate results in this analysis and were not statistically significantly different when compared to mutant or wild-type mice (three heterozygote animals examined at each age, data not shown).

Another measure of refinement is the degree of overlap of contralateral and ipsilateral axons. To quantify overlap, we determined areas containing both contralateral and ipsilateral projections that exceed threshold values (Figures 7O and 7P), using the same data described above. At P5 (Figure 7O), contralateral projections have not retracted significantly from the ipsilateral patch zone, and consequently about 90% of the ipsilateral patch is overlapping, a result very similar between mutant and wild-type mice ($p = 1.0$, ANOVA). At P10 (Figure 7P), both wild-type and mutant projections have partially segregated, but the fraction of ipsilateral patch that remains overlapping in significantly lower in wild-type mice (47%) compared to mutants (66%) ($p = 0.04$, ANOVA). Therefore, the segregation of retinogiculate projections is impaired when CREB expression is reduced. Taken altogether, our analyses suggest that CREB facilitates refinement of retinogeniculate projections and that it may be required for complete and accurate refinement of these projections.

Discussion

A universal feature of vertebrate development is the crucial role of genetic control in the systematic determination of cellular fates and pathways of maturation. Although the roles of transcriptional control in nervous system regionalization and differentiation are well documented, little is known regarding the nuclear regulatory programs that might orchestrate phases of circuit devel-

opment. In this report, we describe the developmental function of a major calcium- and cAMP-regulated transcriptional pathway that is critical for memory consolidation in a variety of systems. Our findings suggest that this pathway, the CRE/CREB transcriptional pathway, operates under spatiotemporal control and is involved in proper activity-dependent refinement of central visual connections in the dorsal thalamus.

Spatiotemporal Control of CREB and CREB Function during Development

Long lasting synaptic modifications are known to require a cascade of nuclear gene expression (for review, see Bailey et al., 1996). A crucial component of the nuclear gene expression cascade is the CRE/CREB transcriptional pathway, a major calcium/cAMP-dependent system in neurons. To examine the regulation of CRE-mediated gene expression during mammalian forebrain development, we used CRE-*lacZ* reporter mice. This in vivo reporter system has been shown to be upregulated in association with experience-dependent plasticity (Barth et al., 2000; Impey et al., 1996; Impey et al., 1998b; Pham et al., 1999). Our findings reported here indicate that CRE/CREB function and CREB protein are highly regulated over the course of development. CRE-mediated gene expression appears transiently during postnatal development of the dorsal thalamus during a period of refinement of thalamic connections. In contrast, cortical CRE-*lacZ* expression largely appears after the first week and remains detectable into adulthood (Barth et al., 2000).

In addition to CRE-mediated gene expression, we found that CREB protein level, CREB protein isoforms, and phospho-CREB are all developmentally controlled. Altogether, these results suggest mechanisms whereby CREB function can be regulated over the course of development. Alternative splicing of the *CREB* message generates a number of CREB protein isoforms (Ruppert et al., 1992). The functional significance of different CREB isoforms is not known, and previously it was believed that the Δ isoform was predominant by far (Blendy et al., 1996; Ruppert et al., 1992). Our present findings indicate that the α isoform is much more abundant in the thalamus during the first postnatal week, suggestive of a developmental role distinct from CREBΔ. By P20, it has declined significantly compared to the Δ isoform. Isoforms of other classes of transcriptional regulators have been described, and in many instances these isoforms have distinct transcriptional activation properties. In *Aplysia*, there is evidence that CREB isoforms comprise a unit of negative and positive regulators that work in concert to control CRE-mediated gene expression (Bartsch et al., 1998). Whether the changing CREBα and CREBΔ levels during mammalian brain development might have functional roles is not yet known.

Genomic Regulation and the Program of Synaptic Remodeling

Experimental work in the plasticity field has focused largely on synaptic mechanisms. However, synapse-specific considerations do not fully account for transitions that occur during neural circuit development, such as critical periods for remodeling and plasticity which are cell-wide processes affecting all synapses. We suggest that these cell-wide processes are controlled at the genomic level, and that the CRE/CREB pathway may be a central mediator of this genomic regulation.

To demonstrate a causal role for CREB in thalamic circuit remodeling, we examined development of retinogeniculate axon projections in transgenic mice with partial deficiency of CREB. The hypomorphic mice have a milder phenotype because of compensation by CREM (CRE modulator protein) and CREBβ, which are upregulated in these mice (Hummler et al., 1994; Blendy et al., 1996). This mouse strain had previously been shown to have partial deficit in long-term memory (Bourtchuladze et al., 1994; Kogan et al., 1997). Our results indicate that refinement of eye-specific sets of projections is incomplete in these mice. The ipsilateral projections remain relatively diffuse in the CREB hypomorphic mice at P10, covering a larger area and overlapping more extensively with contralateral projections. Therefore, these data indicate that CREB contributes to proper refinement of retinogeniculate projections.

The temporal regulation of CRE/CREB is striking, as it coincides with important temporal landmarks during dLGN development. Contralateral retinogeniculate axons reach the dLGN prior to birth, and they have established dense projections by the time ipsilateral connections arrive at P0–P1 (Godement et al., 1984). Strong experimental evidence suggests that activity-dependent, competitive interactions between contralateral and ipsilateral axons cause them to become segregated within the dLGN. However, contralateral axons have an overwhelming advantage by arriving first at the dLGN, and purely competitive mechanisms might lead to the elimination of ipsilateral axons. Therefore, we speculate that the initial phase of retinogeniculate development might be activity independent, and that although contralateral axons have already grown into the dLGN by P1, they have not yet established fully functional synaptic connections. This might allow ipsilateral axons to become established before the phase of competitive refinement begins. We suggest that competitition, refinement, and consolidation of stable synaptic patterns do not happen until after onset of CRE-mediated gene expression, which occurs between P1 and P4. In this scenario, the exact timing of onset of CRE-mediated gene expression in the dLGN is important, since it might determine when competitive interactions between the projections can occur.

Following the stage of retinal axon remodeling, retinogeniculate synapses become highly stable and resistant to alterations in visual experience (Guillery, 1972). During the juvenile stage (which occurs after retinogeniculate refinement), changes in sensory experience can cause profound changes in intracortical synaptic connections, and yet thalamic connections remain resistant to change (Trachtenberg et al., 2000; Wiesel and Hubel, 1963a). Therefore, the critical period for thalamic neural plasticity occurs at an earlier stage compared to cortical plasticity, which can persist into adulthood. What mechanisms might orchestrate the expression and termination of these phases of plasticity, which vary among brain regions? We suggest that differential regulation of CRE-mediated gene expression might play an important role. In prior work, we showed that CRE-mediated gene ex-

pression is induced in the visual cortex, but not in the LGN, in parallel with experience-dependent visual plasticity (Pham et al., 1999). In the present work, we find that thalamic CRE-mediated gene expression ends by P20. Therefore, there are strong correlations between the presence of CRE-mediated gene expression and the potential for synaptic remodeling, indicating that the downregulation of CRE-mediated gene expression with advancing age among different brain regions may terminate critical periods for synaptic reorganization.

CREB Function, Neural Survival, and Circuit Selection during Development

During visual system development, organized neural activity is generated independent of sensory input (for review, see Wong, 1999). Our results indicate that CRE-mediated gene expression occurs in the dLGN prior to vision, and therefore it might be regulated by spontaneous retinal activity. When one eye of the mouse is enucleated at P5, we find that CRE-mediated gene expression is significantly downregulated in the contralateral dLGN. We should note that although work by Weliky and Katz (1999) showed that the dLGN is active in the absence of retinal innervation, this work was done in ferrets and analyzed animals at a more mature stage (P24–P26) compared to our work here. As shown by Penn et al. (1998), anatomic refinement of retinal projections is complete by P9 in the ferret. Our enucleation experiments were performed at a stage when the retinal projections are overlapping (P4–P5). At this stage, it is possible that retinal activity more strongly influences neural activity in the dLGN.

How might the function of CREB in the dLGN, which exerts a cell-wide effect, influence the organization of the developing circuit? We suggest that an important role of CREB at this stage might be to coordinate the remodeling of the developing circuit with the large-scale programmed elimination of neurons that occurs within the forebrain after birth. Because only 70% of dLGN neurons present at birth survive into adulthood (Heumann and Rabinowicz, 1980), decisions must be made regarding which neurons to eliminate and which to retain. It seems likely that mechanisms exist that preferentially eliminate minor members of the circuit, i.e., those that have not established strong connections. CREB is a good candidate to mediate this process because it has been shown to be critical for survival of neurons in vitro (Bonni et al., 1999; Riccio et al., 1999). Consistent with this result, we find that CREB hypomorphic mice have smaller dLGNs than wild-type mice, and fewer cells within the dLGNs. Our data are also consistent with the finding that following bilateral enucleation there is loss of neurons (30% after six months) in the dLGN, compared to age-matched controls (Heumann and Rabinowicz, 1980). Therefore, during development, neurons that have established efficient afferent synaptic connections will fire more strongly, activating CRE-mediated gene expression, and in doing so facilitate their survival.

In summary, the results of this study suggest an important involvement of CREB in the coordination of thalamic circuit development. By exerting spatiotemporal control over cell-wide mechanisms important for synaptic consolidation, CREB may regulate the orderly progression of remodeling that occurs within the thalamus and cortex. The challenge that lies ahead will be to elucidate the mechanisms that control CREB function, to detail the precise cellular functions affected by CREB, and then to identify the downstream molecular components under its coordinate control.

Experimental Procedures

Transgenic Mice

CRE-*lacZ* mice (Impey et al., 1996) were bred and genotyped as described previously (Pham et al., 1999). *CREB* mutant mice (Hummler et al., 1994) were maintained on C57b/6 genetic background as heterozygotes. Because the *CREB* mutation results in few viable offsprings on this background, we crossed a heterozygous male (C57b/6) with a wild-type female (129 background), and the resulting hybrids were used for mating to yield homozygous mice for experimentation. Genotyping was performed by PCR as described previously (Kogan et al., 1997).

Antibodies and Reagents

Sources of antibodies used are as follows: anti-lacZ polyclonal (5′–3′), anti-CREB polyclonal (New England Biolabs), anti-phospho-CREB polyclonal (Upstate Biotechnology), anti-NeuN monoclonal (Chemicon), Rhodamine Red-X anti-rabbit IgG polyclonal (Jackson Immunoresearch), FITC anti-rabbit IgG polyclonal (Jackson), and Alexa 488 anti-FITC polyclonal (Molecular Probes). The tracers Rhodamine and Oregon Green conjugated to dextran amine were from Molecular Probes.

Immunofluorescence

Fluorescence immunohistochemistry for lacZ was performed as described previously (Pham et al., 1999). For CREB and phospho-CREB immunofluorescence, animals were perfused directly with 4% paraformaldehyde (without prior infusion of saline). This is critical because it rapidly stops any changes in phosphorylation state of CREB that might occur. Sixteen micron sections of brain were obtained with a cryostat and then processed via procedures similar to lacZ immunostaining. Binding of CREB or phospho-CREB antibody was performed at room temperature overnight, followed by a secondary antibody (Rhodamine Red X or FITC conjugated anti-rabbit IgG) for 2 hr. For phospho-CREB detection, a third antibody (Alexa 488 anti-FITC) was used to amplify the signal. All imaging was performed using a BioRad confocal microscope.

Western Blotting

Tissue extracts and Western blotting were performed exactly as described previously (Obrietan et al., 1999), with a CREB polyclonal antibody.

Enucleation

CRE-*lacZ* mice were enucleated at P5 and sacrificed at P6. Enucleation was performed by using standard procedures. Twenty-four hours following enucleation, the brain was dissected and freshly frozen (for lacZ immunofluorescence) or perfused (for phospho-CREB). Immunofluorescence and confocal imaging were performed as described above. For quantification, at least two sections per animal were counted and the results averaged. Counts were performed blind to the experimental condition.

Analysis of Retinogeniculate Axons

Injections of fluorescent labeled dextran amine into the eyes of mice were performed as described previously (Antonini et al., 1999). To label sets of projections from each of the two eyes, we used the fluorophores Oregon Green and Rhodamine. After injections, the mice were returned to their cages for 24 hr to allow for transport of the tracers. Then, they were perfused with 4% paraformaldehyde, postfixed for 1 day, and sectioned coronally at 50 μm using a vibrating microtome. Sections that contain the central part of the dLGN were identified by viewing the sections under darkfield. These sections were imaged using a laser-scanning confocal microscope.

This procedure allows both ipsilateral and contralateral retinal projections to be visualized within the same LGN.

For each animal, we imaged and analyzed three sections through the middle of the LGN, which represent the central 30% of the LGN. The area of the dLGN was determined by outlining the perimeter of the contralateral projections using Adobe Photoshop software. The area of the ipsilateral projections was determined using a computer program written in IDL language. The program determines the number of pixels representing ipsilateral projections that exceed a threshold intensity value. To determine the threshold intensity, we must consider the fact that the amount of dye injected into the eye and its uptake by retinal axons is variable between animals. To correct for this variability, we take into account the intensity of labeling of the projections. To compute the threshold intensity, the computer algorithm measures the average intensity of the center of the ipsilateral projections (within an area of 625 pixels), subtracts this from the background intensity taken from a lateral dLGN area (which has no ipsilateral projection), and then half of this value is added to the background value. Therefore, the threshold intensity for ipsilateral projections is defined as the midpoint between the intensity of the central part of the ipsilateral projection and the intensity of the lateral part of the dLGN containing no ipsilateral inputs. This analysis gives a weighted measure of the spread of distribution of the axons. To perform the analysis, it is necessary that the experimenter identify the center of the ipsilateral projection and the background area. To exclude from the pixel count the optic tract and projections in the vLGN (which are labeled), the area of the dLGN is circled and pixels exceeding threshold within this circle counted. Data analyses were performed blind to the genotype of the animals. Statistical analysis was performed by using 2-way analysis of variance (ANOVA).

Analysis of overlap was performed by thresholding both contralateral and ipsilateral projections. Pixels contained in both sets of projections were quantified. Analyses were performed using an algorithm similar to that described above, but were executed using Adobe Photoshop software by a blind observer. Statistical analysis was performed by using 2-way analysis of variance (ANOVA).

Analysis of Geniculate Cell Density

Histologic sections encompassing the central part of the dLGN were stained with cresyl violet. The dLGN was photographed under 100× magnification and recorded digitally. Images were displayed on a computer monitor and cells within an area approximately 0.05 mm^2 in the dorsolateral region of the dLGN were counted. Cell density values of 8 dLGNs per animal were determined and averaged. All measurements were performed blind to genotype of the animals.

Acknowledgments

We are very grateful to Antonella Antonini for her assistance and advice during many phases of this work, to Naoum Issa for assistance with image analysis, and to Joan Russo for help with statistical analysis. We thank also Salwa Al-Noori, Stewart Anderson, Soren Impey, John Neumaier, and Jaime Olavarria for discussions and critical reading of the manuscript. This work was supported by a fellowship from the American Psychiatric Association, start-up funds from the University of Washington, and a NARSAD (National Alliance for Research in Schizophrenia and Depression) Young Investigator Award (all to T.A.P.). We acknowledge grant funding from the National Institutes of Health (to J.L.R.R., A.J.S., D.R.S., and M.P.S.), and from NARSAD and the Nina Ireland Foundation (to J.L.R.R.).

Received October 25, 2000; revised May 3, 2001.

References

Antonini, A., Fagiolini, M., and Stryker, M.P. (1999). Anatomical correlates of functional plasticity in mouse visual cortex. J. Neurosci. *19*, 4388–4406.

Bailey, C.H., Bartsch, D., and Kandel, E.R. (1996). Toward a molecular definition of long-term memory storage. Proc. Natl. Acad. Sci. USA *96*, 13445–13452.

Barth, A.L., McKenna, M., Glazewski, S., Hill, P., Impey, S., Storm, D., and Fox, K. (2000). Upregulation of cAMP response element-mediated gene expression during experience-dependent plasticity in adult neocortex. J. Neurosci. *20*, 4206–4216.

Bartsch, D., Casadio, A., Karl, K.A., Serodio, P., and Kandel, E.R. (1998). CREB1 encodes a nuclear activator, a repressor, and a cytoplasmic modulator that form a regulatory unit critical for long-term facilitation. Cell *95*, 211–223.

Blakemore, C., Garey, L.J., and Vital-Durand, F. (1978). The physiological effects of monocular deprivation and their reversal in the monkey's visual cortex. J. Physiol. *283*, 223–262.

Blendy, J.A., Kaestner, K.H., Schmid, W., Gass, P., and Schutz, G. (1996). Targeting of the CREB gene leads to up-regulation of a novel CREB mRNA isoform. EMBO J. *15*, 1098–1106.

Bonni, A., Brunet, A., West, A.E., Datta, S.R., Takasu, M.A., and Greenberg, M.E. (1999). Cell survival promoted by the Ras-MAPK signaling pathway by transcription-dependent and -independent mechanisms. Science *286*, 1358–1362.

Bourtchuladze, R., Frenguelli, B., Blendy, J., Cioffi, D., Schutz, G., and Silva, A.J. (1994). Deficient long-term memory in mice with a targeted mutation of the cAMP- responsive element-binding protein. Cell *79*, 59–68.

Casadio, A., Martin, K.C., Giustetto, M., Zhu, H., Chen, M., Bartsch, D., Bailey, C.H., and Kandel, E.R. (1999). A transient, neuron-wide form of CREB-mediated long-term facilitation can be stabilized at specific synapses by local protein synthesis. Cell *99*, 221–237.

Corriveau, R.A., Huh, G.S., and Shatz, C.J. (1998). Regulation of class I MHC gene expression in the developing and mature CNS by neural activity. Neuron *21*, 505–520.

Corriveau, R.A., Shatz, C.J., and Nedivi, E. (1999). Dynamic regulation of cpg15 during activity-dependent synaptic development in the mammalian visual system. J. Neurosci. *19*, 7999–8008.

Darian-Smith, C., and Gilbert, C.D. (1995). Topographic reorganization in the striate cortex of the adult cat and monkey is cortically mediated. J. Neurosci. *15*, 1631–1647.

Fagiolini, M., and Hensch, T.K. (2000). Inhibitory threshold for critical-period activation in primary visual cortex. Nature *404*, 183–186.

Fox, K. (1994). The cortical component of experience-dependent synaptic plasticity in the rat barrel cortex. J. Neurosci. *14*, 7665–7679.

Fox, K., and Zahs, K. (1994). Critical period control in sensory cortex. Curr. Opin. Neurobiol. *4*, 112–119.

Fox, K., Daw, N., Sato, H., and Czepita, D. (1991). Dark-rearing delays the loss of NMDA-receptor function in kitten visual cortex. Nature *350*, 342–344.

Galli, L., and Maffei, L. (1988). Spontaneous impulse activity of rat retinal ganglion cells in prenatal life. Science *242*, 90–91.

Godement, P., Salaun, J., and Imbert, M. (1984). Prenatal and postnatal development of retinogeniculate and retinocollicular projections in the mouse. J. Comp. Neurol. *230*, 552–575.

Godement, P., Salaun, J., and Metin, C. (1987). Fate of uncrossed retinal projections following early or late prenatal monocular enucleation in the mouse. J. Comp. Neurol. *255*, 97–109.

Gordon, J.A., and Stryker, M.P. (1996). Experience-dependent plasticity of binocular responses in the primary visual cortex of the mouse. J. Neurosci. *16*, 3274–3286.

Guillery, R.W. (1972). Experiments to determine whether retinogeniculate axons can form translaminar collateral sprouts in the dorsal lateral geniculate nucleus of the cat. J. Comp. Neurol. *146*, 407–420.

Hanover, J.L., Huang, Z.J., Tonegawa, S., and Stryker, M.P. (1999). Brain-derived neurotrophic factor overexpression induces precocious critical period in mouse visual cortex. J. Neurosci. *19*, RC40.

Hardingham, G.E., Chawla, S., Cruzalegui, F.H., and Bading, H. (1999). Control of recruitment and transcription-activating function of CBP determines gene regulation by NMDA receptors and L-type calcium channels. Neuron *22*, 789–798.

Heumann, D., and Rabinowicz, T. (1980). Postnatal development of the dorsal lateral geniculate nucleus in the normal and enucleated albino mouse. Exp. Brain Res. *38*, 75–85.

Hu, S.C., Chrivia, J., and Ghosh, A. (1999). Regulation of CBP-mediated transcription by neuronal calcium signaling. Neuron *22*, 799–808.

Huang, Z.J., Kirkwood, A., Pizzorusso, T., Porciatti, V., Morales, B., Bear, M.F., Maffei, L., and Tonegawa, S. (1999). BDNF regulates the maturation of inhibition and the critical period of plasticity in mouse visual cortex. Cell *98*, 739–755.

Hubel, D.H., and Wiesel, T.N. (1970). The period of susceptibility to the physiological effects of unilateral eye closure in kittens. J. Physiol. *206*, 419–36.

Hubel, D.H., and Wiesel, T.N. (1998). Early exploration of the visual cortex. Neuron *20*, 401–412.

Huh, G.S., Boulanger, L.M., Du, H., Riquelme, P.A., Brotz, T.M., and Shatz, C.J. (2000). Functional requirement for class I MHC in CNS development and plasticity. Science *290*, 2155–2159.

Hummler, E., Cole, T.J., Blendy, J.A., Ganss, R., Aguzzi, A., Schmid, W., Beermann, F., and Schutz, G. (1994). Targeted mutation of the CREB gene: compensation within the CREB/ATF family of transcription factors. Proc. Natl. Acad. Sci. USA *91*, 5647–5651.

Impey, S., Mark, M., Villacres, E.C., Poser, S., Chavkin, C., and Storm, D.R. (1996). Induction of CRE-mediated gene expression by stimuli that generate long- lasting LTP in area CA1 of the hippocampus. Neuron *16*, 973–982.

Impey, S., Obrietan, K., Wong, S.T., Poser, S., Yano, S., Wayman, G., Deloulme, J.C., Chan, G., and Storm, D.R. (1998a). Cross talk between ERK and PKA is required for Ca2+ stimulation of CREB-dependent transcription and ERK nuclear translocation. Neuron *21*, 869–883.

Impey, S., Smith, D.M., Obrietan, K., Donahue, R., Wade, C., and Storm, D.R. (1998b). Stimulation of cAMP response element (CRE)-mediated transcription during contextual learning. Nat. Neurosci. *1*, 595–601.

Katz, L.C., and Shatz, C.J. (1996). Synaptic activity and the construction of cortical circuits. Science *274*, 1133–1138.

Kogan, J.H., Frankland, P.W., Blendy, J.A., Coblentz, J., Marowitz, Z., Schutz, G., and Silva, A.J. (1997). Spaced training induces normal long-term memory in CREB mutant mice. Curr. Biol. *7*, 1–11.

LeVay, S., Stryker, M.P., and Shatz, C.J. (1978). Ocular dominance columns and their development in layer IV of the cat's visual cortex: a quantitative study. J. Comp. Neurol. *179*, 223–244.

Montminy, M. (1997). Transcriptional regulation by cyclic AMP. Annu. Rev. Biochem. *66*, 807–822.

Obrietan, K., Impey, S., Smith, D., Athos, J., and Storm, D.R. (1999). Circadian regulation of cAMP response element-mediated gene expression in the suprachiasmatic nuclei. J. Biol. Chem. *274*, 17748–17756.

Penn, A.A., Riquelme, P.A., Feller, M.B., and Shatz, C.J. (1998). Competition in retinogeniculate patterning driven by spontaneous activity. Science *279*, 2108–2112.

Pham, T.A., Impey, S., Storm, D.R., and Stryker, M.P. (1999). CRE-mediated gene transcription in neocortical neuronal plasticity during the developmental critical period. Neuron *22*, 63–72.

Rakic, P. (1981). Development of visual centers in the primate brain depends on binocular competition before birth. Science *214*, 928–931.

Riccio, A., Ahn, S., Davenport, C.M., Blendy, J.A., and Ginty, D.D. (1999). Mediation by a CREB family transcription factor of NGF-dependent survival of sympathetic neurons. Science *286*, 2358–2361.

Robson, J.A., Mason, C.A., and Guillery, R.W. (1978). Terminal arbors of axons that have formed abnormal connections. Science *201*, 635–637.

Rubenstein, J.L., Martinez, S., Shimamura, K., and Puelles, L. (1994). The embryonic vertebrate forebrain: the prosomeric model. Science *266*, 578–580.

Rudolph, D., Tafuri, A., Gass, P., Hammerling, G.J., Arnold, B., and Schutz, G. (1998). Impaired fetal T cell development and perinatal lethality in mice lacking the cAMP response element binding protein. Proc. Natl. Acad. Sci. USA *95*, 4481–4486.

Ruppert, S., Cole, T.J., Boshart, M., Schmid, E., and Schutz, G. (1992). Multiple mRNA isoforms of the transcription activator protein CREB: generation by alternative splicing and specific expression in primary spermatocytes. EMBO J. *11*, 1503–1512.

Silva, A.J., Kogan, J.H., Frankland, P.W., and Kida, S. (1998). CREB and memory. Annu. Rev. Neurosci. *21*, 127–148.

Sretavan, D.W., and Shatz, C.J. (1986a). Prenatal development of retinal ganglion cell axons: segregation into eye-specific layers within the cat's lateral geniculate nucleus. J. Neurosci. *6*, 234–251.

Sretavan, D.W., and Shatz, C.J. (1986b). Prenatal development of cat retinogeniculate axon arbors in the absence of binocular interactions. J. Neurosci. *6*, 990–1003.

Sretavan, D.W., Shatz, C.J., and Stryker, M.P. (1988). Modification of retinal ganglion cell axon morphology by prenatal infusion of tetrodotoxin. Nature *336*, 468–471.

Trachtenberg, J.T., Trepel, C., and Stryker, M.P. (2000). Rapid extragranular plasticity in the absence of thalamocortical plasticity in the developing primary visual cortex. Science *287*, 2029–2032.

Tsumoto, T., Hagihara, K., and Hata, Y. (1987). NMDA receptors in the visual cortex of young kittens are more effective than those of adult cats. Nature *327*, 513–514.

Upton, A.L., Salichon, N., Lebrand, C., Ravary, A., Blakely, R., Seif, I., and Gaspar, P. (1999). Excess of serotonin (5-HT) alters the segregation of ispilateral and contralateral retinal projections in monoamine oxidase A knock-out mice: possible role of 5-HT uptake in retinal ganglion cells during development. J. Neurosci. *19*, 7007–7024.

Weliky, M., and Katz, L.C. (1999). Correlational structure of spontaneous neuronal activity in the developing lateral geniculate nucleus in vivo. Science *285*, 599–604.

Wiesel, T.N., and Hubel, D.H. (1963a). Effects of visual deprivation on morphology and physiology of cells in the cat's lateral geniculate body. J. Neurophysiol. *26*, 978–993.

Wiesel, T.N., and Hubel, D.H. (1963b). Single-cell responses in striate cortex of kittens deprived of vision in one eye. J. Neurophysiol. *26*, 1003–1017.

Wong, R.O. (1999). Retinal waves and visual system development. Annu. Rev. Neurosci. *22*, 29–47.

Yin, J.C., Wallach, J.S., Del Vecchio, M., Wilder, E.L., Zhou, H., Quinn, W.G., and Tully, T. (1994). Induction of a dominant negative CREB transgene specifically blocks long-term memory in Drosophila. Cell *79*, 49–58.